

Photon-jet coincidence measurements in polarized pp collisions at $\sqrt{s} = 200$ GeV with the STAR Endcap Calorimeter

Ilya Selyuzhenkov for the STAR Collaboration

Indiana University Cyclotron Facility, 2401 Milo B. Sampson Lane, Bloomington, IN 47408, USA

Abstract. Recent inclusive measurements with polarized proton-proton collisions at RHIC provide significant constraints on the polarized gluon distribution, $\Delta g(x)$, integrated over the gluon momentum range $0.02 < x < 0.3$. Di-jet and photon-jet coincidence measurements will allow to study the x -dependence of $\Delta g(x)$. In this report we present the status of photon-jet coincidence studies for photons detected at forward pseudorapidity, $1.08 < \eta < 2$, using the STAR Endcap Calorimeter.

Keywords: polarized pp collisions, polarized gluon distribution, photon-jet coincidence

PACS: 12.38.-t, 13.85.-t, 13.87.-a, 13.88.+e, 14.70.Bh, 24.70.+s, 24.85.+p

Introduction. Recent results from RHIC for the inclusive jet [1] and π^0 [2] double spin asymmetry A_{LL} at mid-rapidity provide significant constraints [3] on the integral of the polarized gluon distribution over the gluon momentum range $0.02 < x < 0.3$. Information on the gluon spin distribution as a function of x , $\Delta g(x)$, will add insight if the observed smallness of the integral value originates from possible cancellations. It is also of great importance to extrapolations over unmeasured regions of x . Determining the $\Delta g(x)$ dependence requires reconstruction of the initial-state parton kinematics, which can be achieved with di-jet or photon-jet coincidence measurements. The photon-jet channel is dominated by a single partonic subprocess (quark-gluon Compton scattering), and through measurement of the photon energy and direction, along with the jet direction, allows more precise reconstruction of the parton kinematics. In this report we present the status of our photon-jet coincidence studies for photons detected at forward rapidity, $1.08 < \eta < 2$, using the STAR Endcap Electro-Magnetic Calorimeter (EMC) [4]. Full jet reconstruction at mid-rapidity, $|\eta| < 0.8$, is obtained using the STAR Time Projection Chamber (TPC) [5] and the Barrel EMC detectors [6].

Data samples, event selection, and uncorrected yields. Our analysis is based on an integrated luminosity of 3.1pb^{-1} longitudinally polarized proton-proton collisions at $\sqrt{s} = 200$ GeV which were recorded with the STAR detector during year 2006. The trigger required at least one 2×2 cluster of towers in the Endcap EMC with transverse energy greater than 5.2 GeV and transverse energy of the associated tower above 3.7 GeV. Two event samples (signal and background) of simulated pp collisions were used for detailed study of trigger and detector biases, and to derive purity of the extracted signal. Events were generated using PYTHIA 6.4 [7] with parameters adjusted to CDF "Tune A" settings [8] in the parton transverse momentum range 2-25 GeV. The signal rate is calculated based on simulated PYTHIA prompt photon production processes.

Physics backgrounds are studied with PYTHIA QCD hard scattering two parton production processes. Realistic response of the STAR detector is simulated with the GEANT 3 Monte-Carlo package [9] with full trigger emulation. The generated luminosity for each Monte-Carlo sample is comparable to that of the data: 7pb^{-1} for direct photon-jet, and 1pb^{-1} for QCD background samples.

All events were processed with the midpoint-cone jet finding algorithm [10], and only those with exactly two jets which pointed back-to-back in azimuth, $\cos(\phi_{jet} - \phi_\gamma) < -0.8$, were selected for the analysis. The photon candidate is defined as the jet with the maximum neutral energy, and its energy is calculated based on the 3×3 cluster of Endcap EMC towers centered around the tower of highest energy. Additional event fiducial cuts on the photon candidate pseudo-rapidity $1.08 < \eta_\gamma < 2$ and transverse momentum $p_T^\gamma > 7$ GeV, and on the away-side jet $|\eta_{jet}| < 0.8$ and $p_T^{jet} > 5$ GeV were applied. Figure 1(a) shows acceptance and efficiency uncorrected

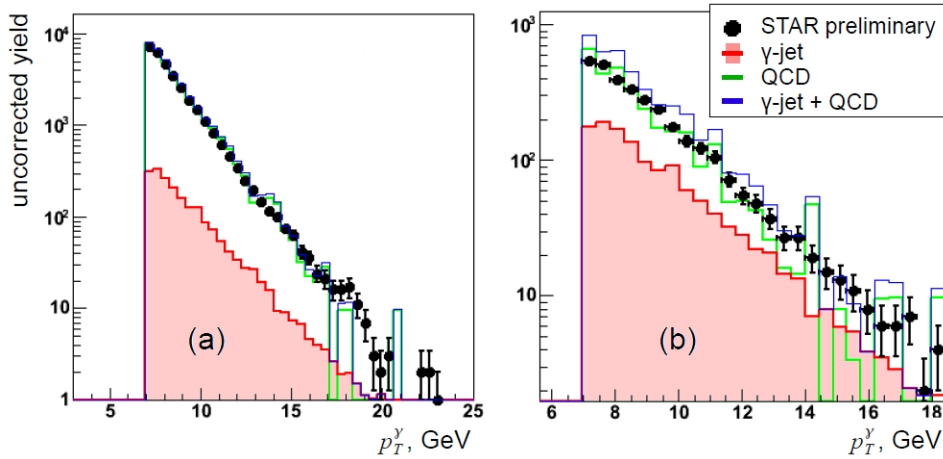


FIGURE 1. Uncorrected yields vs. photon candidate transverse momentum. Black circles indicate the yield of photon-jet candidates from STAR run 6 pp collisions at $\sqrt{s} = 200$ GeV, red (green) lines show simulated prompt photons (QCD background) yield, and blue lines represent sum of the simulated yields.

yields for data and simulation samples after applying event fiducial cuts. The sum of the simulated yields were normalized to the yield in data. Figure 1(b) shows uncorrected yields after background suppression according to the photon-jet isolation procedure discussed below.

Transverse shower profile and photon-jet isolation. The main source of physics background in the direct photon measurement originates from multi-photon production processes, such as $\pi^0 \rightarrow \gamma\gamma$ decay. In this study, for multi-photon discrimination we used the STAR Endcap Shower Maximum Detector (SMD) [4]. High SMD granularity allows for precise photon position reconstruction, while SMD strip energy deposition provides important information on the transverse electromagnetic shower profile. For the shower shape study and cut optimization, all events were pre-sorted into four different categories based on energy deposition in the two Endcap EMC pre-shower layers: (a) $E_{pre1} = E_{pre2} = 0$; (b) $E_{pre1} = 0, E_{pre2} > 0$; (c) $0 < E_{pre1} < 4$ MeV; and (d) $4 < E_{pre1} < 10$ MeV. Here $E_{pre1(2)}$ is the pre-shower energy deposition under the 3×3 cluster of towers.

Figure 2 shows the average energy deposition per SMD strip vs. relative distance to the

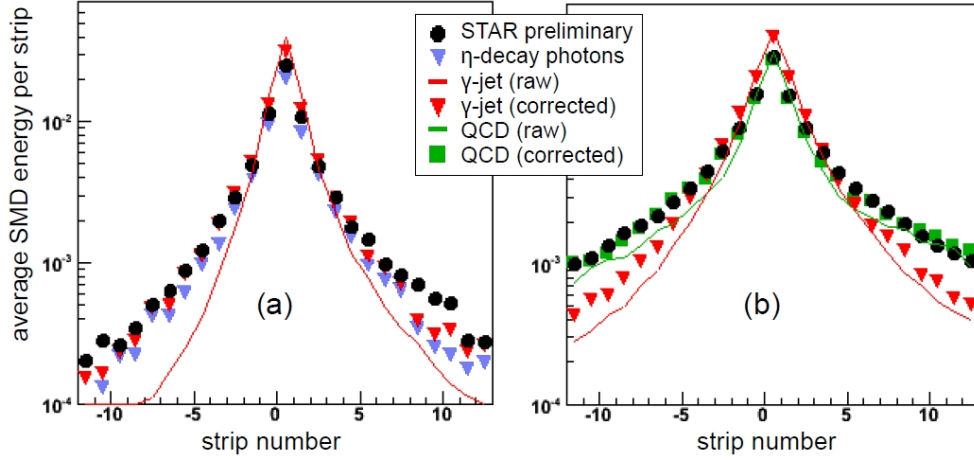


FIGURE 2. Photon candidate transverse shower profiles. Black circles present shower shapes from real pp collisions at $\sqrt{s} = 200$ GeV. Red (green) lines correspond to simulated prompt photon (QCD background) shower shapes, while red triangles (green squares) indicate shower profiles from data-driven simulations (see text for details).

strip of highest energy (strip number). Figure 2(a) shows the transverse energy profile for a sample of events with $E_{pre1} = E_{pre2} = 0$ (direct photon rich), while Fig. 2(b) presents a sample with $4 < E_{pre1} < 10$ MeV (background dominated). From Fig. 2 it is clear that GEANT Monte-Carlo with the STAR run 6 geometry generates transverse shower profiles which are not consistent with those from the real data (compare red or green line vs. black circles in Fig. 2). This disagreement has been fixed by event-by-event substitution of the GEANT simulated SMD response for each of the Monte-Carlo photons with that of isolated photons from real data. To build a library of real photon shower shapes, we used a sample of reconstructed η -mesons which decayed into two well-separated photons such that their showers do not overlap in SMD. Shower shapes from this so-called data-driven simulation are indicated in Fig. 2 by red triangles (direct photon) and green squares (QCD background). For comparison, the transverse shower profile of single photons from η -meson decay is shown as blue triangles.

Direct photon shower shapes were parametrized with a triple Gaussian function which was used to fit the SMD response in data and simulation on an event-by-event basis. For each event, the fit results are subtracted from the observed SMD energy deposition, and the extra energy on each side of the SMD peak is calculated. The maximum of these energies (maximum sided-residual) is further used for multi-photon background discrimination. In addition, the following event information is used for background suppression: (a) energy fraction of the 3×3 tower cluster within a larger ($r = 0.7$) radius in $\Delta\eta \times \Delta\phi$; (b) number of Endcap EMC towers fired around photon candidate within $r = 0.7$; (c) number of Barrel EMC towers fired around photon candidate within $r = 0.7$; (d) number of charged tracks reconstructed with the TPC around photon candidate within $r = 0.7$; (e) photon and jet transverse momentum balance, $[p_T^\gamma - p_T^{jet}]/p_T^\gamma$; (f) post-shower energy deposition for the 3×3 cluster of Endcap EMC towers. For this set of discriminating variables, the cuts were optimized with a Linear Discriminant Analysis (LDA) [11]. Given i discriminating variables, v_i , the LDA assigns a specific weight, w_i ,

and all variables are combined into a single linear discriminant: $D = \sum_i v_i w_i$. The LDA optimizes weights in such a way that signal and background discriminant distributions are pushed as far as possible away from each other. Figure 3 shows the result of weight

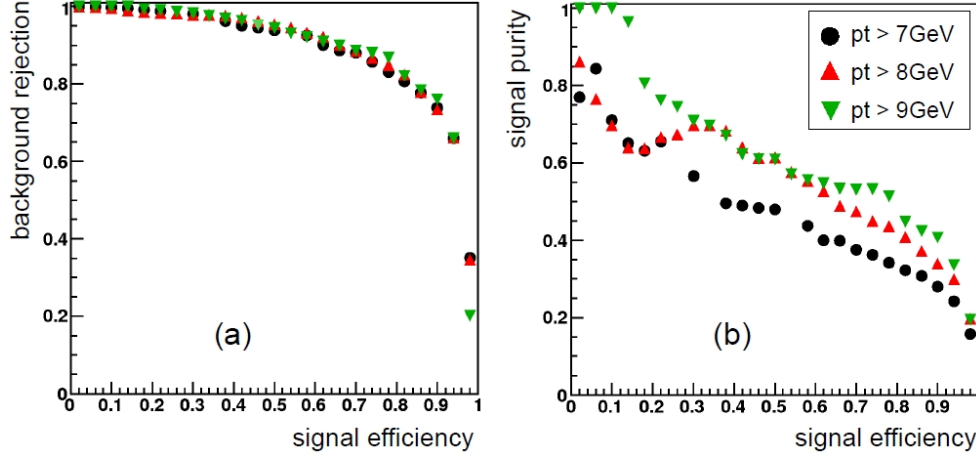


FIGURE 3. (a) Background rejection vs. signal efficiency. (b) Signal purity vs. signal efficiency. Results are shown for the $E_{pre1} = 0, E_{pre2} > 0$ pre-shower condition.

optimization with LDA for three different cuts on the photon transverse momentum: $p_T^\gamma > 7, 8,$ and 9 GeV. As can be seen from Fig. 3(b), for a given efficiency of 70% and the $E_{pre1} = 0, E_{pre2} > 0$ condition we can reach 40% purity in $p_T^\gamma > 7$ GeV range. As a function of p_T^γ , signal purity averaged over all pre-shower conditions varies between 25-40% (corresponding uncorrected yields are shown in Fig. 1(b)).

Summary. The status of photon-jet coincidence studies for photons detected at forward rapidity, $1.08 < \eta < 2$, using the STAR detector is presented. Depending on the photon transverse momentum, we have reached 25-40% overall purity of the photon-jet sample. This result is an important step towards calculation of the total photon-jet cross section in the photon rapidity range $|\eta_\gamma| > 1$. With the statistics collected by STAR during this year's run 9, this should allow for statistically significant double spin asymmetry measurements with photon-jet coincidences.

REFERENCES

1. B. I. Abelev *et al.* [STAR Collaboration], Phys. Rev. Lett. **100**, 232003 (2008).
2. A. Adare *et al.* [PHENIX Collaboration], arXiv:0810.0694 [hep-ex]; Phys. Rev. D **79** (2009) 012003.
3. D. de Florian, R. Sassot, M. Stratmann and W. Vogelsang, Phys. Rev. Lett. **101**, 072001 (2008); arXiv:0904.3821 [hep-ph] and references therein.
4. C. E. Allgower *et al.* [STAR Collaboration], Nucl. Instrum. Meth. A **499**, 740 (2003).
5. M. Anderson *et al.*, Nucl. Instrum. Meth. A **499**, 659 (2003) [arXiv:nucl-ex/0301015].
6. M. Beddo *et al.* [STAR Collaboration], Nucl. Instrum. Meth. A **499**, 725 (2003).
7. T. Sjostrand, S. Mrenna and P. Skands, JHEP **0605**, 026 (2006) [arXiv:hep-ph/0603175].
8. R. Field and R. C. Group [CDF Collaboration], arXiv:hep-ph/0510198.
9. Geant 3.21, CERN Program Library.
10. G. C. Blazey *et al.*, arXiv:hep-ex/0005012.
11. A. Hocker *et al.*, PoS A CAT, 040 (2007) [arXiv:physics/0703039].